The Astrophysical Journal, 739:68 (10pp), 2011 October 1 doi:10.1088/0004-637X/739/2/68

PTF1 J071912.13+485834.0: AN OUTBURSTING AM CVn SYSTEM DISCOVERED BY A SYNOPTIC SURVEY

David Levitan[1], Benjamin J. Fulton[2], Paul J. Groot[3,4], Shrinivas R. Kulkarni[4], Eran O. Ofek[4,10], Thomas A. Prince[1], Avi Shporer[2,5], Joshua S. Bloom[6], S. Bradley Cenko[6], Mansi M. Kasliwal[4], Nicholas M. Law[7], Peter E. Nugent[8], Dovi Poznanski[6,8,10], Robert M. Quimby[4], Assaf Horesh[4], Branimir Sesar[4], and Assaf Sternberg[9]
[1] Division of Physics, Mathematics, and Astronomy, California Institute of Technology, Pasadena, CA 91125, USA
[2] Las Cumbres Observatory Global Telescope Network, 6740 Cortona Drive, Suite 102, Santa Barbara, CA 93117, USA
[3] Department of Astrophysics, IMAPP, Radboud University Nijmegen, P.O. Box 9010, NL-6500 GL Nijmegen, The Netherlands
[4] Cahill Center for Astrophysics, California Institute of Technology, Pasadena, CA 91125, USA
[5] Department of Physics, Broida Hall, University of California, Santa Barbara, CA 93106, USA
[6] Department of Astronomy, University of California, Berkeley, CA 94720-3411, USA
[7] Dunlap Institute for Astronomy and Astrophysics, University of Toronto, 50 St. George Street, Toronto, M5S 3H4 Ontario, Canada
[8] Computational Cosmology Center, Lawrence Berkeley National Laboratory, 1 Cyclotron Road, Berkeley, CA 94720, USA
[9] Benoziyo Center for Astrophysics, Faculty of Physics, Weizmann Institute of Science, Rehovot 76100, Israel
Received 2011 May 9; accepted 2011 July 6; published 2011 September 7

ABSTRACT

We present extensive photometric and spectroscopic observations of PTF1 J071912.13+485834.0, an outbursting AM CVn system discovered by the Palomar Transient Factory (PTF). AM CVn systems are stellar binaries with some of the smallest separations known and orbital periods ranging from 5 to 65 minutes. They are believed to be composed of a white dwarf accretor and a (semi-)degenerate He-rich donor and are considered to be the helium equivalents of cataclysmic variables (CVs). We have spectroscopically and photometrically identified an orbital period of 26.77 ± 0.02 minutes for PTF1 J071912.13+485834.0 and found a super-outburst recurrence time of greater than 65 days along with the presence of "normal" outbursts—rarely seen in AM CVn systems but well known in super-outbursting CVs. We present a long-term light curve over two super-cycles as well as high-cadence photometry of both outburst and quiescent stages, both of which show clear variability. We also compare both the outburst and quiescent spectra of PTF1 J071912.13+485834.0 to other known AM CVn systems, and use the quiescent phase-resolved spectroscopy to determine the origin of the photometric variability. Finally, we draw parallels between the different subclasses of SU UMa-type CVs and outbursting AM CVn systems. We conclude by predicting that the PTF may more than double the number of outbursting AM CVn systems known, which would greatly increase our understanding of AM CVn systems.

Key words: accretion, accretion disks – binaries: close – novae, cataclysmic variables – stars: individual (PTF1 J071912.13+485834.0) – white dwarfs

1. INTRODUCTION

AM CVn systems—ultra-compact semi-detached binaries—are stellar binaries with some of the smallest separations known. They have been found with orbital periods ranging from 5 to 65 minutes. The prototype, AM CVn, was initially identified as a possible binary star by Smak (1967) and was eventually theorized to be composed of a relatively massive white dwarf accretor and a much lower mass semi-degenerate or degenerate helium-transferring donor (Paczyński 1967; Faulkner et al. 1972). AM CVn systems are believed to be one of the strongest Galactic low-frequency gravitational wave sources (Nelemans et al. 2004; Roelofs et al. 2007b) and the source of the proposed ".Ia" supernovae (Bildsten et al. 2007). We refer the reader to Nelemans (2005) and Solheim (2010) for reviews.

Short-period systems—those with orbital periods below roughly 20 minutes—are in a constant state of high mass transfer from the secondary to the optically thick accretion disk. They are known as "high" state systems, and their spectra, dominated by the accretion disk, are characterized by broad, shallow helium absorption lines with few other features. High-state systems have been observed to have superhumps—photometric variability of ∼0.1 mag with a period slightly longer than the orbital period (e.g., Patterson et al. 1997)—similar to those found in SU UMa-type cataclysmic variables (CVs; Osaki 1996).

At the other end of the period range are the quiescent systems with orbital periods above roughly 40 minutes. They are believed to have low mass-transfer rates and an optically thin disk. Instead of absorption lines, these systems have prominent helium emission lines in their spectra. Quiescent systems do not show prominent photometric variability.

Between these two period ranges are the so-called outbursting AM CVn systems, which feature outbursts similar to those found in dwarf novae-type CVs. While in the "high" state, these systems exhibit the properties of short-period AM CVn systems, and while in the "quiescent" state, they exhibit properties of the long-period AM CVn systems (see, e.g., Roelofs et al. 2007a). In outburst they are typically 3–5 mag brighter than in quiescence and feature superhumps. These outbursts tend to last for a few weeks, and recur on a timescale (where known) between 46 days (e.g., Kato et al. 2000) and over a year (e.g., Copperwheat et al. 2011). Between the two states, some of these systems have been observed to have a "cycling" state wherein some experience magnitude changes of ∼1 mag with a period of about a day (Patterson et al. 2000). One system, CR Boo, has also been found to have "normal" outbursts that last 1–2 days and recur every 4–8 days (Kato et al. 2000), as opposed to the longer "super-outbursts" described previously.

AM CVn systems have been extensively compared to CVs. Of primary interest for this comparison are the SU UMa-type dwarf novae-type CVs, which exhibit both super-outbursts and normal outbursts, but with somewhat longer typical recurrence

[10] Einstein fellow.

times than outbursting AM CVn systems. See Warner (1995) for an extensive review. While the photometric behavior is similar between dwarf novae and AM CVn systems, the chemical composition, structure of the donor, and evolutionary pathways are very different.

Only 26 AM CVn systems have been reported in the literature. Being intrinsically rare and with colors similar to those of ordinary white dwarfs, they are difficult to discover and population estimates have proven to be difficult to calculate (e.g., Nelemans et al. 2001; Roelofs et al. 2007b). Initially, AM CVn systems were serendipitous discoveries, typically as a result of their photometric variability or color. More recently, the population has almost doubled as a result of the Sloan Digital Sky Survey (SDSS). Seven systems were discovered from a search for spectra containing helium emission lines (Roelofs et al. 2005; Anderson et al. 2005, 2008) and five more from a follow-up color selection and spectroscopic survey (Roelofs et al. 2009; Rau et al. 2010).

However, the wide variety of photometric variability exhibited by AM CVn systems makes them an effective target for large-scale, synoptic surveys. The most recent published new AM CVn system, with an orbital period of 15.6 minutes, was discovered in *Kepler* satellite data from its superhump-induced photometric variability (Fontaine et al. 2011). Here, we present a new AM CVn system discovered in outburst by the Palomar Transient Factory (PTF)—the first system discovered by a systematic, synoptic survey covering thousands of square degrees.

The PTF[11] uses the Oschin 48 inch telescope (P48) at the Palomar Observatory to image 7.2 deg^2 with each exposure. In a typical night, up to ∼2000 deg^2 are observed to a depth of $R \sim 20.6$ (Law et al. 2009; Rau et al. 2009).

We begin by describing the discovery of PTF1 J071912.13+485834.0[12] (hereafter PTF1J0719+4858) and summarizing our follow-up observations. In Section 3, we present photometric observations. We describe the features of both outburst and quiescent spectra in Section 4, as well as the determination of the spectroscopic period from phase-resolved spectroscopy. In Section 5, we compare PTF1J0719+4858 to other outbursting AM CVn systems, discuss the source of the quiescent photometric variability, and consider how many more such systems can be discovered by PTF. Finally, we summarize in Section 6.

2. DISCOVERY AND SUMMARY OF OBSERVATIONS

PTF1J0719+4858 was detected in outburst by the PTF at $R = 15.8$ on 2009 December 1 and classified as a transient with the designation PTF09hpk.[13] A graphical summary of the PTF photometry can be found in Figure 1.

A classification spectrum was taken using Keck-I/LRIS (Low Resolution Imaging Spectrometer) (McCarthy et al. 1998) on 2010 January 14 and reduced using standard IRAF tasks. Noticing the lack of a redshift, the PTF extragalactic team classified the spectrum as a CV. In a subsequent inspection of the PTF spectral database, we noticed the presence of multiple distinct, double-peaked helium emission lines, some with a central peak (we refer the reader to Section 4.2 which contains a high signal-to-noise quiescence spectrum), and it was reclassified as an AM CVn system candidate.

[11] http://www.astro.caltech.edu/ptf.

[12] "PTF1" refers to preliminary versions of the PTF catalog, as opposed to sources from the final catalog, which will use "PTF." It is possible that a source in the PTF1 catalog will have slightly different coordinates in the PTF catalog.

[13] This is a PTF transient designation. For stellar discoveries, we use the more conventional IAU variable star coordinate name.

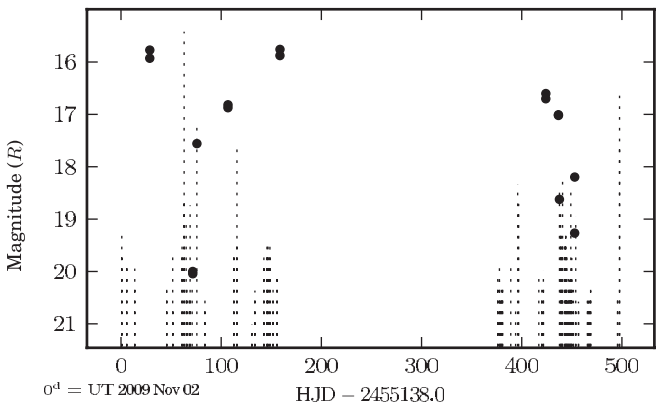

Figure 1. PTF light curve of PTF1J0719+4858. Discovery occurred at the first data point. Magnitudes were obtained by difference imaging relative to a deep co-added reference image as part of the PTF Transient Pipeline. The tops of the dashed lines represent limits for non-detections and are theoretical calculations based on observed conditions. Errors on observations in outburst are ∼0.01 mag and errors in quiescence are ∼0.1 mag. Note that these observations are in the R band as opposed to the g' band used in the rest of this paper. PTF1J0719+4858 is a blue object and hence fainter in R.

We focused our follow-up efforts on both long-term monitoring and short-timescale variability studies, using the Palomar 60 inch telescope (P60) and two telescopes from the Las Cumbres Observatory Global Telescope Network (LCOGT; Shporer et al. 2010): the 2 m Faulkes Telescope North (FTN) and the 32 inch Byrne Observatory at Sedgwick (BOS). Between 2010 October and 2011 March, we obtained a total of 195 exposures in good weather for our long-term photometric monitoring campaign using P60 and FTN with a goal of obtaining at least one exposure per night. We present this light curve in Section 3.2. We also observed PTF1J0719+4858 at high cadence several times to characterize the photometric variability on the order of the orbital period, both in quiescence and in outburst. We discuss the periods identified from these observations in Section 3.3.

Besides photometric observations, we also obtained individual spectra of PTF1J0719+4858 on multiple nights, as well as phase-resolved spectroscopy. Individual spectra of PTF1J0719+4858 were obtained with Keck-I, the William Herschel Telescope (WHT), and the Palomar 200 inch Hale Telescope in 2010 October and November. To obtain the orbital period, we obtained roughly four hours of spectroscopic observations with Keck-I/LRIS using three-minute exposures. These observations are presented in Section 4.2.

3. PHOTOMETRIC OBSERVATIONS AND RESULTS

3.1. Analysis and Reduction Process

Palomar 60 inch data were de-biased and flat-fielded using the P60 pipeline (Cenko et al. 2006). The FTN data were processed using the LCOGT pipeline. The BOS data were de-biased and flat-fielded using IRAF tasks, astrometrically calibrated using Astrometry.net (Lang et al. 2010), and cosmic rays were removed using the L.A. Cosmic algorithm (van Dokkum 2001). The Sextractor package (Bertin & Arnouts 1996) was used to identify sources in each exposure and their instrumental magnitudes were obtained using optimal point-spread function photometry (Naylor 1998) as implemented by the Starlink[14] package autophotom.

[14] The Starlink Software Group homepage can be found at http://starlink.jach.hawaii.edu/starlink.

Light curves were calculated using a matrix-based, least-squares minimization, relative photometry algorithm. The primary goal of any such algorithm is to minimize noise, typically by assuming certain stars in the field are non-variable and identifying an optimal zero point for each exposure. We expanded on this to simultaneously solve for both the zero point and additional de-trending terms that corrected for airmass and instrument changes. The algorithm is similar to that developed in Honeycutt (1992) and is described in the Appendix of Ofek et al. (2011).

To accomplish the de-trending, we modeled each observation as

$$m_{i,j} = \overline{M}_j + Z_i + \alpha c_j A_i + \sum_{k=1}^{n_k} \beta_k c_j,$$

where the data needed are as follows.

1. $m_{i,j}$: the magnitude of source j on exposure i.
2. c_j: a color for each source. The color is required to compensate for the stronger effects of airmass on blue stars, as well as the differences in CCD efficiency over a range of wavelengths. For our light curves, we used $c_j = g'_j - r'_j$, where g'_j and r'_j refer to the magnitudes of the jth source in the respective SDSS filters.
3. A_i: the airmass of each exposure.

The terms to be fitted are as follows.

1. Z_i: the optimal zero-point term of each exposure.
2. $\overline{M}_j$: the mean magnitude term of the source.
3. α: the airmass calibration coefficient for all exposures and sources.
4. β_k: the kth telescope/instrument calibration coefficient, for $k = 1, 2, \ldots, n_k$ where n_k is the number of telescopes. This term is introduced to take into account the different responses of each telescope/instrument. For light curves with data from only one instrument, these terms were not used.

It is important to ensure that all stars used for the solution (calibration stars) are themselves not variable. We restricted the stars used to those found in 80%–100% of exposures, depending on the light curve, and iteratively removed any sources with high residuals. Since the solution is not unique unless reference magnitudes are provided, we used blue magnitudes from USNO-B 1.0.

This algorithm provided very good results—even light curves taken over months with different telescopes and conditions obtained a magnitude scatter (rms) of ∼0.035 mag for $g' \approx 16$ and ∼0.055 mag for $g' \approx 19.4$, the quiescent magnitude of PTF1J0719+4858. The rms errors provided with the figures in this paper are based on the median scatter of other stars with similar magnitude present in at least 50% of observations. Additionally, individual errors—the combination of the Poisson error and the fit errors—are provided for some of the light curves. These are typically very close to the magnitude scatter, except for those exposures obtained during bad weather.

For high-cadence light curves, period analysis was performed with SigSpec (Reegen 2007). All default options were used, except as noted for individual cases, and weights for measurements were always provided. SigSpec produces a list of significant periods and corresponding "sig" values. A "sig" value of c means that the period has a chance of 1 in 10^c of being noise.

3.2. Long-term Photometric Behavior

The long-term light curve of PTF1J0719+4858 from FTN and P60 is presented in Figure 2. We note the pattern of "high" states and "quiescent" states. Additionally, we note the presence of "normal" outbursts (as opposed to the "super-outbursts" more commonly associated with AM CVn systems).

We observed the 2011 January super-outburst in its entirety and find a rise time from the last measurement in quiescence to the peak magnitude of 3.2 days with Δmag = 3.6. Immediately following this rise, we see a drop to a plateau that may be the cycling state seen in other AM CVn systems (e.g., Patterson et al. 2000). Finally, 22 days after the beginning of the super-outburst, PTF1J0719+4858 returned to quiescence.

The recurrence time was significantly different between the two super-cycles we observed. We approximate (assuming the behavior of the super-outburst itself is the same) that the recurrence time from the first super-outburst to the second was 65 days. However, the recurrence time from the second super-outburst to the third is greater than 78 days (this uncertainty is due to weather impacting our observations).

Between super-outbursts, we observed normal outbursts in PTF1J0719+4858, which have also been identified in CR Boo (Kato et al. 2000). After initially observing single data points indicating a sudden jump in luminosity, we successfully predicted the 2011 January 29 outburst and obtained a total of 41 exposures, of which 12 are from BOS and are not included in the long-term light curve. The light curve of this outburst is presented in Figure 3. During this normal outburst, PTF1J0719+4858 experienced a luminosity increase of 2.5 mag over 7 hr from the last observation at $g' > 19.4$ to the brightest point measured. If we consider only the increase from $g' > 19$ we find an increase of 2.1 mag over only 4 hr.

The recurrence time of the normal outbursts was stable throughout the first super-cycle. We observed three normal outbursts with a recurrence time of ∼10.5 days. This most likely represents all the normal outbursts in this super-cycle, due to our almost daily coverage. The delay between the end of the second super-cycle and the first normal outburst was the same as that in the first super-cycle. However, it appears that the normal outburst recurrence time was significantly different in the second super-cycle, likely associated with the longer recurrence time of the super-outburst. Given our poor coverage (as a result of weather), we cannot make any statements about these differences.

3.3. High-cadence Photometry

Short-term photometric variability was detected in several high-cadence observations of PTF1J0719+4858 (see Table 1 and labels in Figure 2).

During the first super-outburst (labeled HC1), we detected photometric variability of Δmag ≈ 0.1 (see Figure 4) with a shape consistent with that of superhumps in other AM CVn systems (e.g., Patterson et al. 1997; Wood et al. 2002). Analysis of the period using a Lomb–Scargle periodogram suggests it is ∼27 minutes, while a SigSpec analysis found a period of ∼26 minutes. Given that we observed only two cycles, we cannot state a more accurate superhump period.

A second set of high-cadence observations (labeled HC2) was obtained almost immediately after PTF1J0719+4858 returned to quiescence following the first observed super-outburst. Here, we see photometric variability of Δmag ≈ 0.2. We performed a SigSpec analysis of the light curve for these two nights with the AntiAIC anti-aliasing feature enabled and found a period of

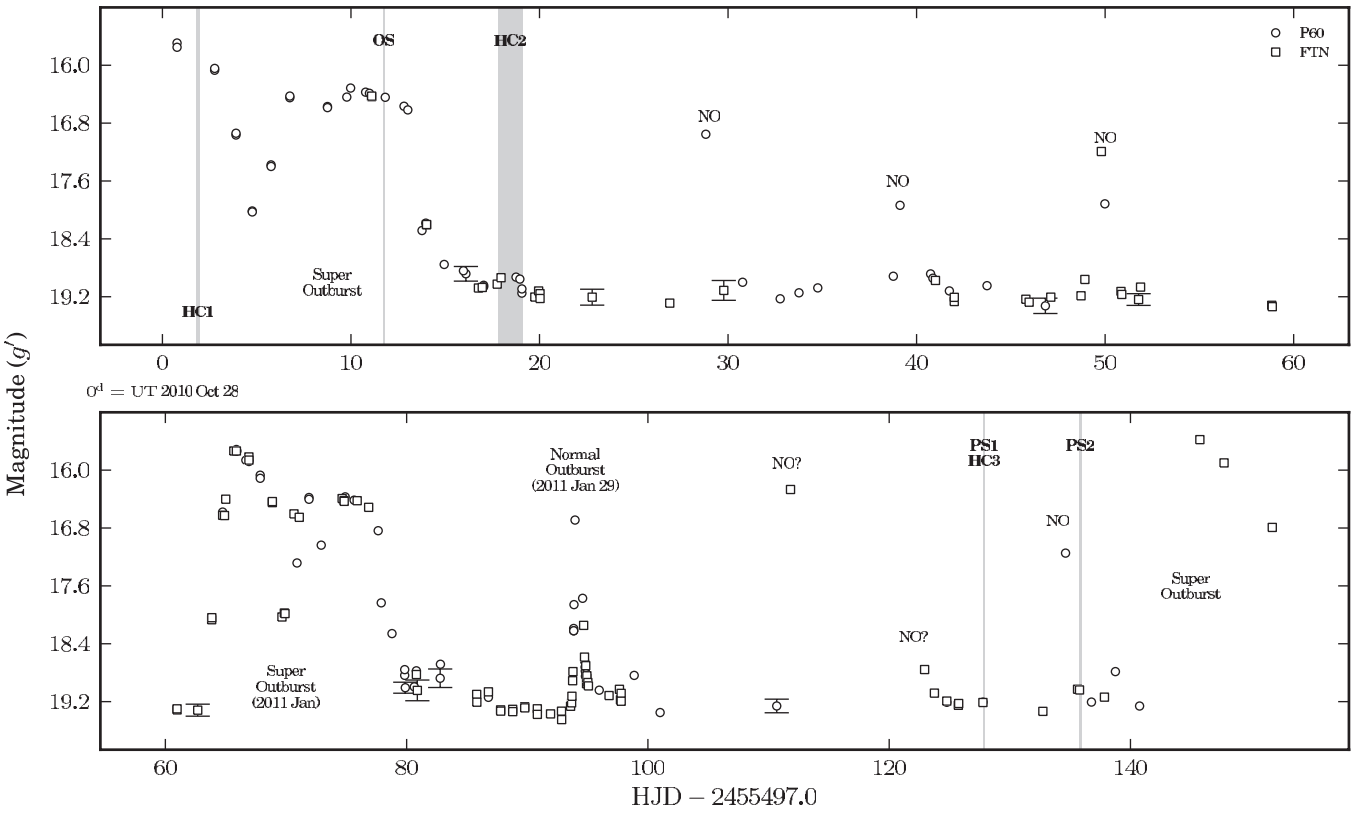

Figure 2. Long-term light curve of PTF1J0719+4858 with 90 exposures from P60 and 105 exposures from FTN. Exposures from both telescopes were 60 s and we attempted to obtain 1–2 exposures per night. Twenty-nine calibration stars were used to achieve an rms of ∼0.055 mag in quiescence and an rms of ∼0.035 mag in outburst (small enough that the error bars cannot be seen). Observations with $\sigma > 0.075$ mag (due to weather or other issues) are marked with error bars. Note the difference in the scale of the time axis for the upper and lower panels: the top half shows the first super-outburst cycle (∼60 days) and the bottom half shows the second cycle (∼80 days). The 2011 January super-outburst (the only one observed in its entirety) is labeled as is the normal outburst of 2011 January 29. The other data points we believe to be normal outbursts are labeled as NO. Two of these points are questionable due to lack of observations and are identified with a question mark. The quiescent magnitude is $g' \approx 19.4$. The high-cadence runs in Table 1 are identified as HC*n* while the phase-resolved spectroscopy runs discussed in Section 4.2 are identified as PS*n*. The outburst spectrum discussed in Section 4.1 is labeled as OS.

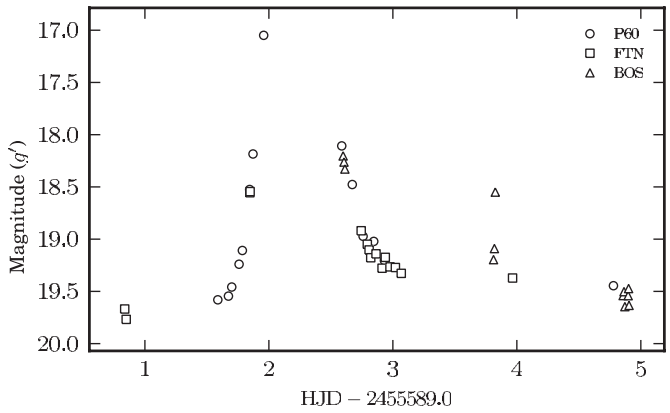

Figure 3. Normal outburst of PTF1J0719+4858 (2011 January 29). The light curve contains 41 exposures, with 14 from P60 (60 s), 15 from FTN (60 s), and 12 from BOS (300 s). Forty-five calibration stars were used. At $g' \approx 17$, rms ≈ 0.02 mag and at $g' \approx 19.5$, rms ≈ 0.04 mag.

1606.3 ± 2.5 s with a "sig" of 13.7. Since we observed many periods of this variability, we present a phase-binned light curve in Figure 5. Additional observations that allow a more precise determination of the superhump period could be used along with the quiescent photometric period to determine a mass ratio (Patterson et al. 2005).

We also obtained a set of high-cadence observations (labeled HC3) coincident with our phase-resolved spectroscopy at Keck-I (see Section 4.2). These observations also showed photometric variability, with Δmag ≈ 0.06. PTF1J0719+4858 was in quiescence at the time of the observations. A SigSpec analysis identified a period of 1550 s with a sig of 3.1. Given the short observation time and the low significance, we folded the light curve at both this period and the spectroscopic period obtained in Section 4.2. These produced similar results and, thus, we believe that the true period is that obtained via phase-resolved spectroscopy. We discuss the simultaneous photometry and spectroscopy in Section 5.2.

Table 1
High-cadence Photometry Runs of PTF1J0719+4858

Label	Telescope	UT Date(s)	Exposures	Read-out Time (s)
HC1	P60	2010 Oct 29	92 × 45 s	10[a]
HC2	BOS	2010 Nov 14/15	54/60 × 300 s	31
HC3	P60	2011 Mar 4	87 × 60 s	24

Notes. All exposures taken with a g' filter.
[a] Taken in quarter-chip mode, which decreased read-out time.

4. SPECTROSCOPIC OBSERVATIONS AND RESULTS

4.1. Follow-up Spectra

The identification spectra were reduced as part of the PTF spectroscopic program using standard IRAF tasks. We present

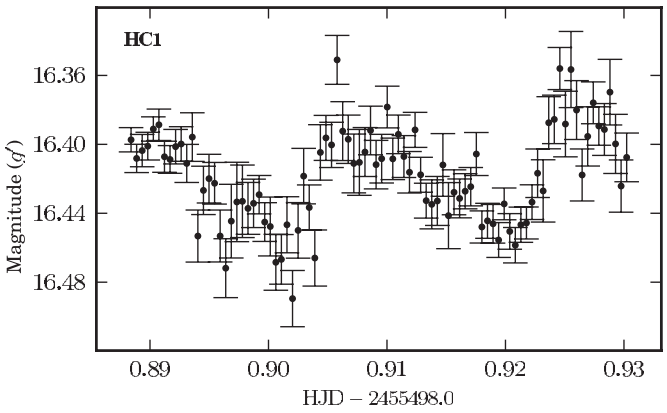

Figure 4. Superhumps of PTF1J0719+4858. The light curve was constructed using 12 calibration stars, and other sources at this magnitude had an rms of ∼0.015 mag. The shape is consistent with superhumps in similar systems such as CR Boo (Patterson et al. 1997) and KL Dra (Wood et al. 2002).

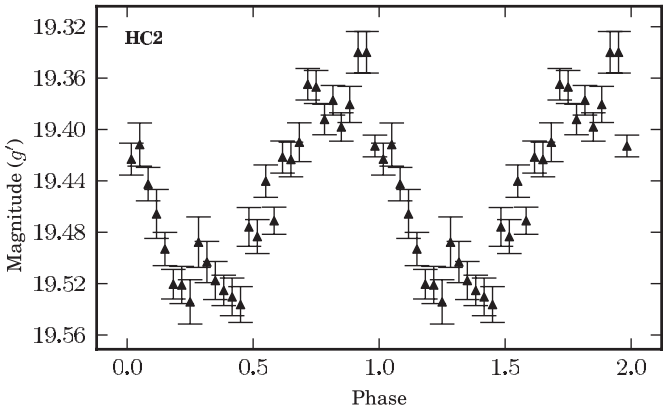

Figure 5. Phase-binned light curve of PTF1J0712+4858 in quiescence from 114 BOS exposures of 300 s folded on a period of 1606.3 s. Eighteen calibration stars were used to construct the light curve. At this magnitude, rms ≈ 0.035 mag. Error bars for individual points are based on the standard deviation of all measurements in that phase bin. An arbitrary zero phase of HJD = 2455514.831555 (the start of the observations) was used.

Table 2
Equivalent Widths of Identified Lines from Co-added Quiescence Spectrum

Line	Equivalent Width (Å)
He I λ4387	−4.9 ± 0.1
He I λ4471	−9.4 ± 0.1
He II λ4686 + He I λ4713	−9.8 ± 0.3
He I λ4921	−3.7 ± 0.1
He I λ5015 + 5047	−5.2 ± 0.2
He I λ5876	−14.7 ± 0.3
He I λ6678	−10.7 ± 0.4
He I λ7065	−7.2 ± 0.4

Table 3
Phase-resolved Spectroscopy Using Keck-I/LRIS

UT Date	CCD	Disp. Elem.	Bins[a]	Slit (″)	Exposures
2011 Mar 4	Blue	600/4000	4 × 4	1.5	37 × 180 s
2011 Mar 4	Red	600/7500	4 × 4	1.5	35 × 180 s
2011 Mar 12	Blue	600/4000	4 × 2	0.7	32 × 180 s
2011 Mar 12	Red	600/7500	4 × 2	0.7	30 × 180 s

Notes. Binning was increased to reduce read-out noise and time. The conditions were substantially better on 2011 March 12, allowing the use of less binning in the spatial direction.
[a] Spectral × spatial.

a typical outburst spectrum—taken with WHT/ACAM (Benn et al. 2008) on 2010 November 6 and labeled as OS in Figure 2—in Figure 6 with the prominent lines identified. The outburst spectra varied slightly, with absorption lines being more prominent on some than on others. However, He I λ4471 was always visible. The best spectrum in quiescence is the co-added spectrum of the phase-resolved observations, shown in Figure 7, again with lines identified.

The quiescence spectrum features very broad, double-peaked emission lines, some with a possible central spike. Shortward of 4000 Å, the spectrum shows an interplay of lines that is consistent with Ca II H and K emission interwoven with He I λ3888 (see Roelofs et al. 2006a), but the low resolution of the current observation and the broadness of the lines make their presence difficult to establish. We can establish the presence of Fe II, Si, and N I emission lines in the rest of the spectrum. It is also possible that He II λ4200 is seen in the spectrum, albeit very weak. He II λ4200 has not been previously seen in an AM CVn system. In the outburst spectrum, we see weak absorption lines of He I and He II, as well as Fe II. Si is not seen, but we note the presence of N I λ8223, which has not been seen this strong in other high-state AM CVn systems.

Table 2 lists the equivalent widths of the most prominent emission lines. Based on the presence of the noted elements, we find that the spectra of PTF1J0719+4858 are most similar to those of 2003aw (Roelofs et al. 2006a) and SDSSJ0804+1616 (Roelofs et al. 2009). Future work in identifying abundances may shed light on the chemical composition and evolutionary history of such systems (Nelemans et al. 2010).

4.2. High-speed Spectroscopy in Quiescence

Here, we discuss the phase-resolved spectroscopy undertaken at the Keck Observatory (see Table 3). The spectra were reduced using optimal extraction (Horne 1986) as implemented in the Pamela code (Marsh 1989) as well as the Starlink packages kappa, figaro, and convert. For these exposures, wavelength calibration exposures were taken at the beginning, middle, and end of each set of observations using the Hg, Cd, and Zn lamps for the blue CCD and the Ne and Ar lamps for the red CCD. Wavelength calibration for individual spectra was interpolated between these calibration spectra. We present a co-added spectrum in Figure 7.

We use a technique similar to previous analyses of AM CVn system phase-resolved spectra, first developed by Nather et al. (1981), to establish the orbital period. Each spectrum was re-binned to the same wavelengths and the locations of individual emission lines were identified. Because of the large number of cosmic rays on the red side despite processing with L.A. Cosmic (van Dokkum 2001), we concentrated on the blue side and used the helium lines at 4026 Å, 4387 Å, 4471 Å, 4686 Å, 4921 Å, and 5015 Å. The lines from each exposure were re-binned and co-added to produce a summed He emission line. We then subtracted the red 40% of the line from the blue 40% of the line, and divided by the continuum. This produced a time series of flux ratios, which we analyzed using SigSpec. We identified a period of 1606.2 ± 0.9 s with a "sig" of 3.1. The statistical significance spectrum is in Figure 8.

While not a very high confidence level, we believe the above period is, in fact, the orbital period, for two reasons. First, the period found is within the error bars of the previously discussed

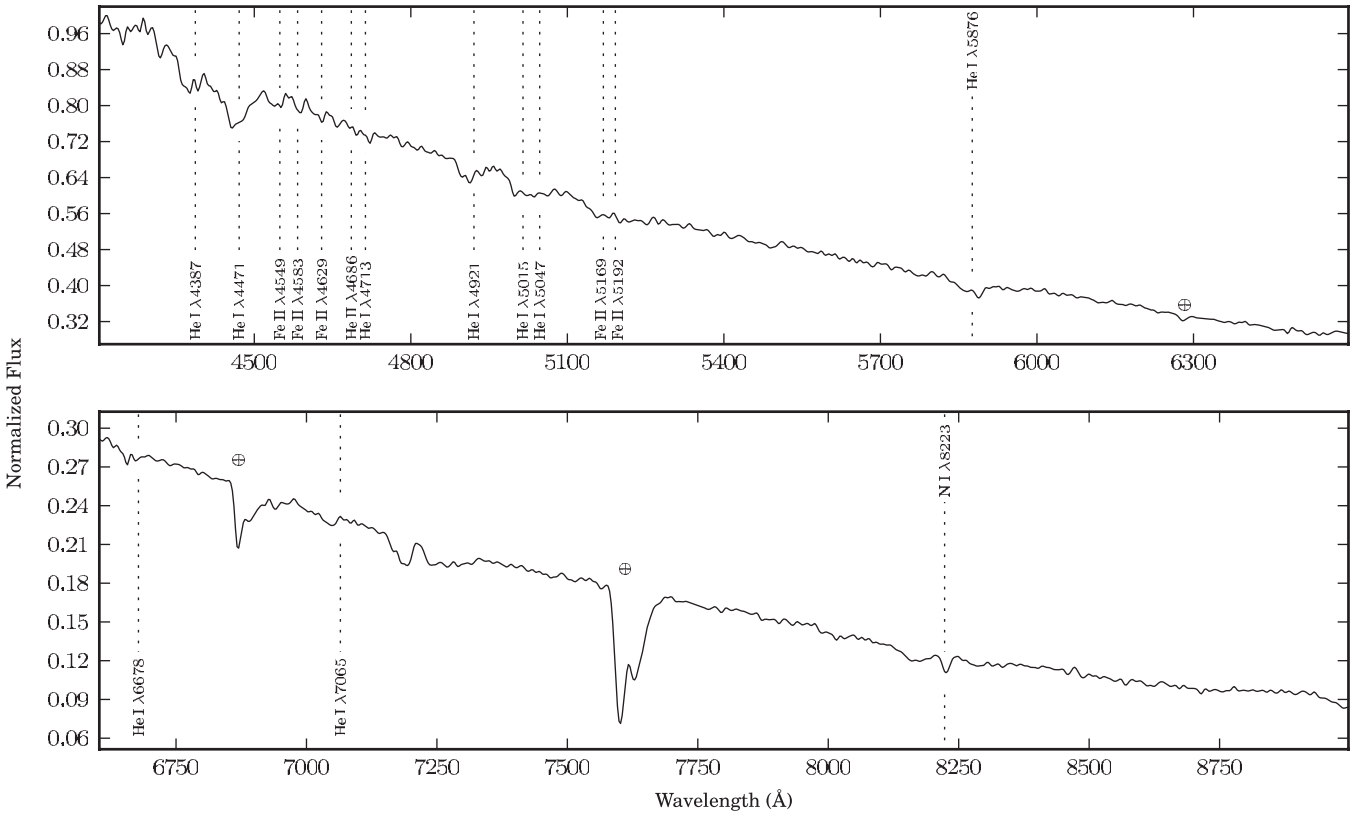

Figure 6. Outburst spectrum of PTF1J0719+4858 taken with WHT/ACAM on 2010 November 6. Strong helium absorption lines are present throughout the spectrum, as well as Fe II lines. We also highlight the N I λ8223 absorption line, which has not been seen before in an AM CVn system in the high state.

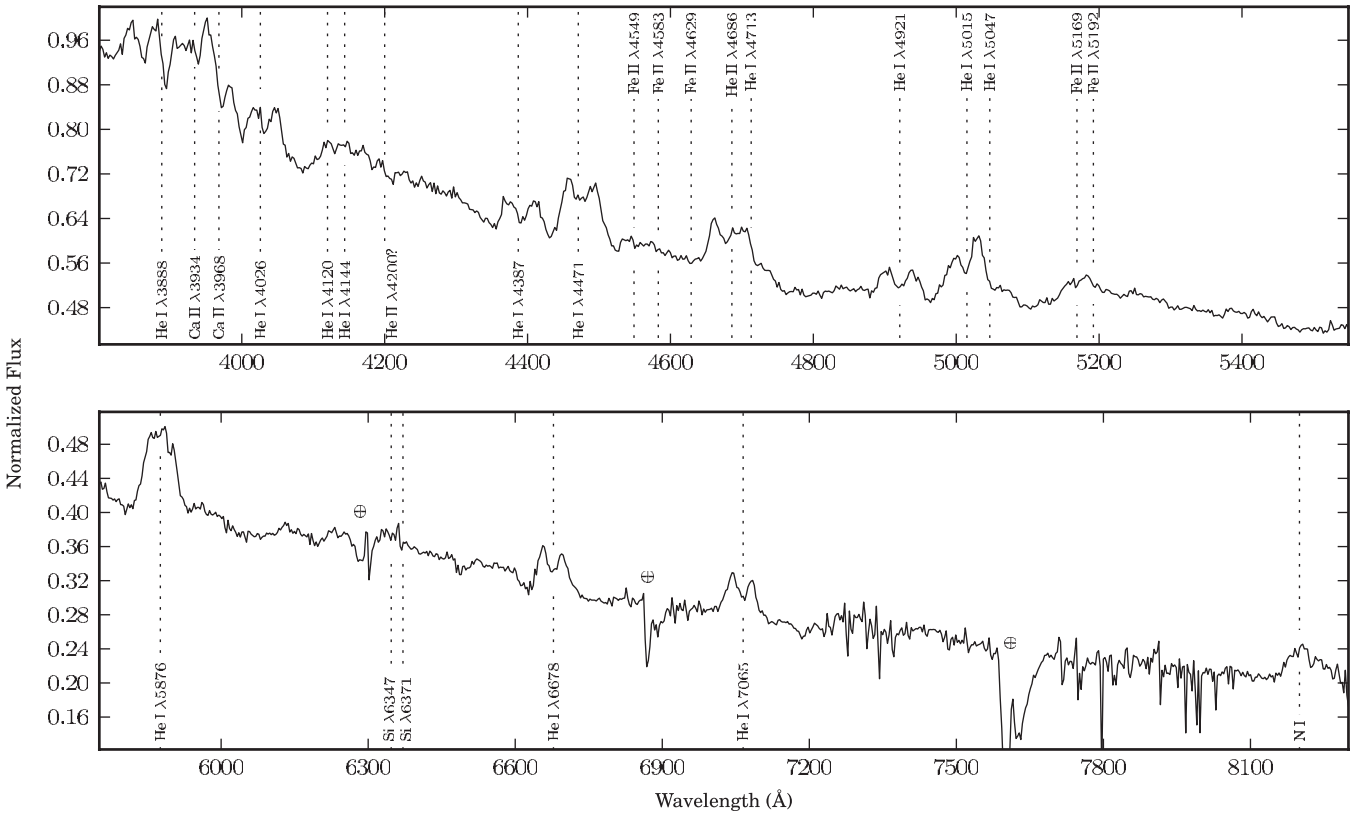

Figure 7. Co-added Keck-I/LRIS quiescence spectrum of PTF1J0719+4858. A total of 72 exposures of 180 s were co-added for the blue side. For the red side, 62 exposures of 180 s were median co-added to remove cosmic-ray effects. Strong helium lines are evident, along with Fe II and Si λ6347 + 6371. A broad emission feature of N I is also present at ∼8200 Å.

Table 4
Properties of Known Outbursting AM CVn Systems

Object	Orbital Period (s)	Super-outburst Recurrence Time (days)	Δmag	References
CR Boo	1471	46.3[a]	4.5	Kato et al. (2000, 2001)
KL Dra	1500	50	4.2	Wood et al. (2002); D. Levitan et al. (2011, in preparation)
V803 Cen	1596	77	4.6	Nogami et al. (2004); Roelofs et al. (2007a)
PTF1J0719+4858	1606	65–80	3.5	This paper
SDSSJ0926+3624	1699	104–449	3.3	Copperwheat et al. (2011)
CP Eri	1701	...[b]	3.2	Abbott et al. (1992); Groot et al. (2001)
2003aw	2028	...[b]	4.8	Nogami et al. (2004); Roelofs et al. (2006a)
2QZ J1427−01	2194[c]	...[b]	5.3	Woudt et al. (2005)
SDSSJ1240−0159	2241	...[b]	4.5	Roelofs et al. (2005); P. A. Woudt (2005, private communication); Shears et al. (2011)
SDSSJ0129+3842	2274[c]	...[b]	4.6	Anderson et al. (2005); Shears et al. (2011)
SDSSJ2047+0008	...	...[b]	∼6	Anderson et al. (2008)

Notes.
[a] Reported as 46.3 days in Kato et al. (2000), but reported as variable in Kato et al. (2001) based on additional data.
[b] These systems have no published recurrence time, but it is believed to be significantly longer than 3 months.
[c] Superhump period.

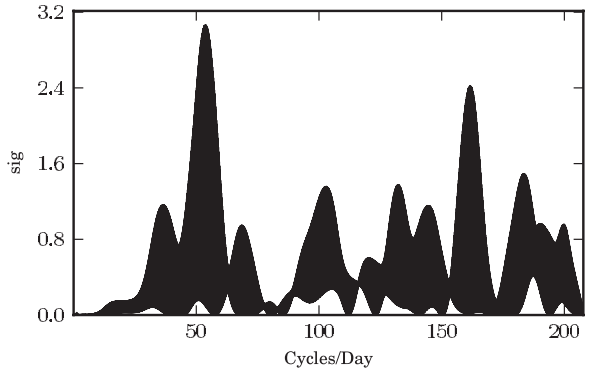

Figure 8. Signficance spectrum of helium emission line flux ratios obtained from Keck-I/LRIS phase-resolved spectroscopy on 2011 March 4/12 (generated by SigSpec).

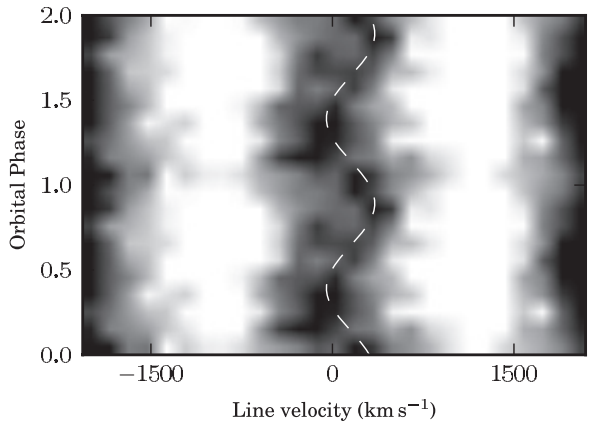

Figure 9. Phase-folded, trailed spectrum of the combined He emission lines visible on Keck-I/LRIS's blue CCD. The period is set to 1606.2 s. The "S-wave," marked by a dashed line, is faint but present. Variation in gray scale indicates relative flux densities. The two white columns are the double-peaked structure of the He emission lines. The start of the first night of observations, at HJD = 2455624.81212, was used as the zero phase.

quiescent photometric period (see Section 3.3). Second, the movement of the disk's hot spot can be identified by creating a phase-binned, trailed spectrum of the He emission line. The rotation of the disk produces an "S-wave" that has been observed previously in known systems (e.g., Roelofs et al. 2005; Rau et al. 2010). In the case of PTF1J0719+4858, this S-wave is very weak, but still discernible. We present the trailed spectrum in Figure 9. This is not the first system where the S-wave was difficult to detect. As reported in Roelofs et al. (2009), an S-wave in SDSSJ0804+1616 was not found in one of two sets of spectra. Further observations are required to establish whether PTF1J0719+4858 has similar variability in the strength of the S-wave or if it is simply a weak feature.

5. DISCUSSION

5.1. Comparison of Long-term Light Curve with that of Other AM CVn Systems

We broadly group the known outbursting AM CVn systems into two categories: those having super-outbursts that occur at least every three months and those with less frequent super-outbursts. The latter group has either poorly determined or undetermined recurrence times. We summarize their properties in Table 4.

It appears that these sources can be cleanly divided by orbital period, with the break between 1606 s and 1699 s. For the first group, the recurrence times are fairly well determined and appear to correlate with the orbital period. The second group is more difficult to understand, primarily due to a lack of known recurrence times. The one published recurrence time, for SDSSJ0926, is very poorly determined (Copperwheat et al. 2011). However, there does appear to be a clear gap between the determined recurrence times of PTF1J0719+4858 and the much more poorly determined recurrence time of SDSSJ0926+3624, and we question whether this difference in recurrence time is purely a result of the increased orbital period (and thus decreased mass-transfer rates) or if different parameters also place a role (such as the mass of the primary and/or the entropy of the secondary).

We can draw parallels to the much more common CVs. The class of CVs most like outbursting AM CVn systems are the SU UMa-type CVs, which also exhibit both normal outbursts and super-outbursts with superhumps (Warner 1995). SU UMa-type systems typically have super-outburst recurrence times

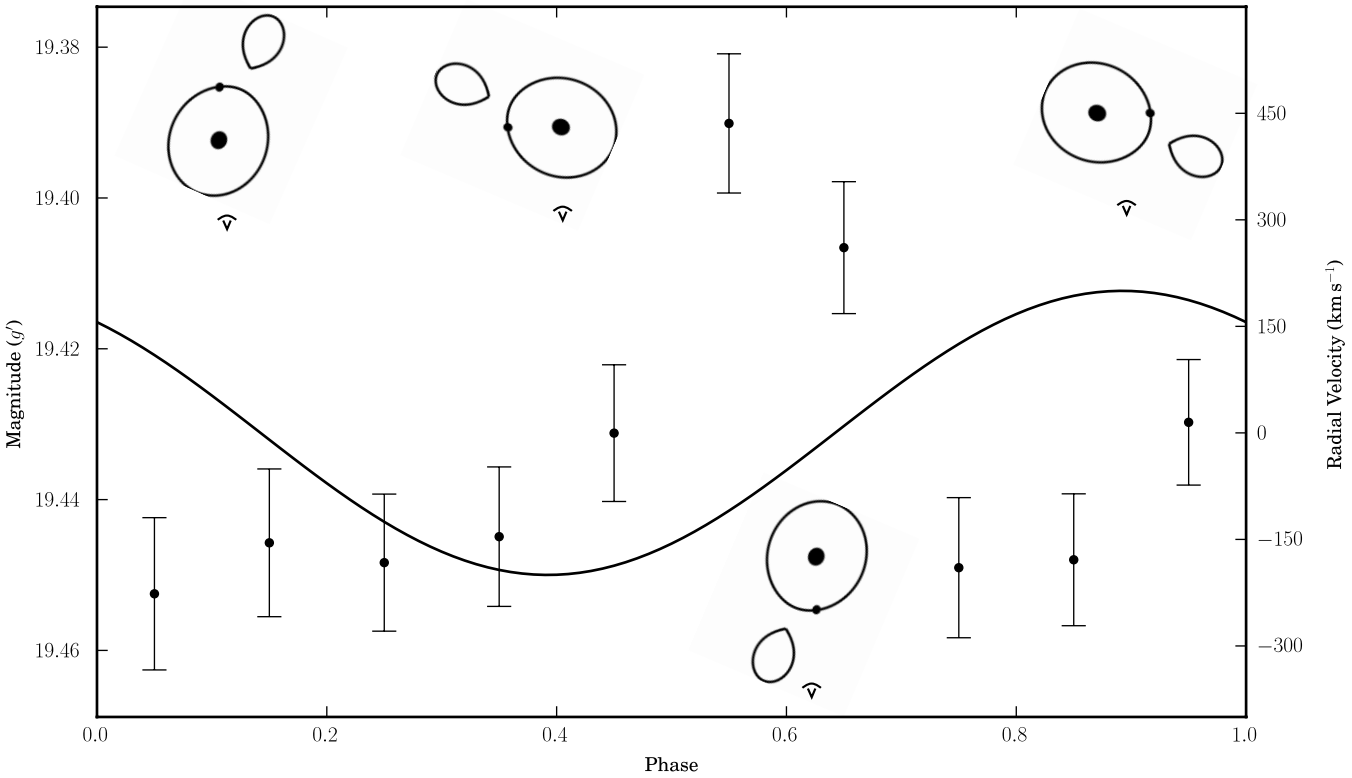

Figure 10. Phase-binned light curve taken on 2011 March 4 using the P60. Eighty-seven 60 s exposures were binned into 10 bins with a zero phase of HJD = 2455624.81212, the start of the phase-resolved spectroscopy, and the spectroscopically derived period of 26.77 minutes. Overplotted is the S-wave found in Section 4.2. The rough orientation of the binary is shown with drawings at the four extreme points of the orbit, along with the position of the observer. We see that the increase in brightness is coincident with the radial velocity of the hot spot being roughly zero and the time period preceding it, indicating that the hot spot and the previously heated disk edge is the likely source of the increased brightness.

of several hundred days and orbital periods between 90 and 120 minutes (Osaki 1996), but have been found to have two extreme cases. The ER UMa-type systems have recurrence times between 19 and 45 days (Buat-Ménard & Hameury 2002), while WZ Sge-type systems have recurrence times of decades and lower orbital periods of 80–90 minutes. The long recurrence times of WZ Sge-type systems are explained by the lower mass-transfer rates of WZ Sge-type systems, as a result of their more evolved state (CVs are believed to have negative $\dot{P}$, as opposed to AM CVn systems; Osaki 1996).

In Kato et al. (2000), CR Boo was proposed to be the helium equivalent of an ER UMa-type CV. However, given that all four of the frequently outbursting systems appear to have fairly similar behavior, we believe that this is typical behavior for AM CVn systems with these orbital periods, as opposed to an extreme case. On the other hand, the recurrence times of the longer period outbursting AM CVn systems indicate that these systems are more akin to the WZ Sge-type CVs. This is consistent with the assumption that AM CVn systems have positive $\dot{P}$ and thus have lower mass transfer with greater orbital periods. Additional discoveries of AM CVn systems, as well as better, more systematic observations of known systems, are necessary to understand the reality of the difference in recurrence times.

5.2. Origin of Photometric Variability in Quiescence

The high-cadence photometric observations discussed in Section 3.3 and labeled as HC3 were coincident with the phase-resolved spectroscopy discussed in Section 4.2, providing us with an opportunity to determine the source of the observed photometric variability. We present a binned, phase-folded photometric light curve in Figure 10, together with the radial velocity of the hot spot. The binning provides an increase in the signal-to-noise and gives a roughly 5σ detection. We remind the reader that HC3 was observed in quiescence, during which time superhumps are not believed to occur in either AM CVn systems or CVs.

The increase in brightness immediately follows the blueshifted portion of the radial velocity curve and is coincident with a lack of radial velocity. This indicates that the photometric variability in PTF1J0719+4858 is caused by the hot spot and the associated heated edge of the disk being closest to the observer (see drawings in Figure 10). We assume here that the S-wave is, in fact, caused by the hot spot.

AM CVn system variability in quiescence has been observed for other non-eclipsing systems such as CR Boo (Provencal et al. 1997) and KL Dra (Wood et al. 2002), but no study has been done of the origin. However, such studies for CVs have linked the hot spot to the observed photometric variability (e.g., Schoembs & Hartmann 1983).

The concern with this explanation is the lack of precision in the photometric data and the lack of time resolution as a result of the binning. This also makes it difficult to compare Figure 10 to observations of other AM CVn systems or CVs. However, we believe that there is sufficient data to link the quiescent variability to the location of the hot spot relative to the observer.

5.3. Potential for Future Discoveries with PTF

How many additional AM CVn systems might be discovered by PTF? First, we estimate the fraction of all AM CVn systems

that are outbursting. Consider a simple model of a single system's evolution by assuming that gravitational wave radiation and angular momentum loss from mass transfer are solely responsible for the evolution of the orbital period (Paczyński 1967; Nelemans et al. 2001). Then, using typical mass values for an AM CVn system at its minimum period ($0.6\,M_{\odot}$ and $0.25M_{\odot}$, although similar values do not significantly affect the results) we find that an AM CVn system spends ∼0.5% of its life between orbital periods of 20 and 27 minutes (the frequent outbursters) and ∼3.3% of its life between orbital periods of 27 and 40 minutes (the less frequent outbursters). We use these numbers as a simple estimate of the percentage of AM CVn systems that are outbursting.

We now estimate the number of systems PTF could discover. Given that AM CVn systems have outbursts with $\Delta\mathrm{mag} \gtrsim 3$, we conservatively assume that any outbursting system with a quiescent magnitude of $\lesssim$23 can be detected in outburst by PTF. We assume a scale height of 300 pc (Roelofs et al. 2007b) and a scale length of 2.5 kpc (Sackett 1997) in the Galaxy and an AM CVn system space density of $\rho_o = 3.1 \times 10^{-6}$ pc^{-3} (the observed space density based on pessimistic population models from Roelofs et al. 2007b). Given that the systems are in quiescence, we further assume that the accretor provides all of the system's luminosity, and use Equation (5) from Roelofs et al. (2007b), which is a parameterization of Figure 2 in Bildsten et al. (2006), to calculate the absolute magnitudes of the AM CVn systems. This likely means that our estimate is conservative since the disk is known to provide part of the luminosity (∼30% for SDSSJ0926+3624; see Marsh et al. 2007) in quiescence. We find that there are approximately $\frac{1.3\ \mathrm{systems}}{100\ \mathrm{deg}^2}$ with orbital periods between 20 and 40 minutes and at $20^{\circ} < |b| < 60^{\circ}$ (the galactic latitudes for most of PTF's observations). Given PTF's footprint of 10,000 deg^2, we estimate that PTF might detect up to 136 such systems. However, the uncertainty in the AM CVn system population density estimates likely means that this number is only accurate to within a factor of 10.

However, the apparent long outburst recurrence times of longer period systems will make these much more difficult to detect. If we consider only those systems with frequent outbursts and thus orbital periods between 20 and 27 minutes, we find that there are up to 18 such systems. Given the recurrence times of 45–80 days, the presence of normal outbursts in at least two systems, and the super-outburst duty cycle of 30%–50%, it is very likely that all 18 systems can be detected as part of the PTF transient search.

We note that searches in lower galactic latitudes make detection much more likely. The population distribution of outbursting AM CVn systems almost doubles between $20^{\circ} < |b| < 25^{\circ}$ and $15^{\circ} < |b| < 20^{\circ}$. Although the analysis of lower-latitude data is more difficult due to the larger number of sources overall, it still presents the best opportunity to discover a large number of AM CVn systems.

Despite the exciting possibilities of using synoptic surveys to search for outbursting systems with quiescent magnitudes up to $R \sim$ 23–25 (and even deeper for future surveys), we caution that confirmation of these systems will be difficult. The established method for finding orbital periods is via phase-resolved spectroscopy, requiring large telescopes and short exposure times for even fairly bright objects. Even objects with a quiescent magnitude of $R \sim 23$ cannot be observed in such a fashion with today's telescopes. Instead, such systems can be observed in outburst. The hot spot has been observed in high-state AM CVn systems (Roelofs et al. 2006b) and it is likely that it can be seen in the high state of outbursting systems as well. Additionally, as demonstrated with PTF1J0719+4858 and other AM CVn systems, photometric periods can be obtained from both superhumps and (potentially) in quiescence, providing a good estimate of the orbital period.

6. SUMMARY

We have presented extensive photometric and spectroscopic observations of PTF1 J071912.13+485834.0. We have observed the system in both quiescence and outburst, observing the strong emission lines and a weak photometric period in the former, and absorption lines and detectable superhumps in the latter. From the phase-resolved spectroscopy, we have identified a weak, albeit detectable, signal in the spectrum that indicates an orbital period of 1606.2 ± 0.9 s. These data, in combination with the simultaneous high-cadence photometry, have allowed us to determine the possible source of the quiescent photometric variability. We also have looked at the long-term light curve and found a variable super-outburst recurrence time, as well as regularly occurring normal outbursts. Based on the identified spectroscopic period, the double-peaked emission lines in quiescence, and its photometric behavior, we classify PTF1J0719+4858 as an AM CVn system.

PTF1J0719+4858 has the longest orbital period of known, frequently outbursting AM CVn systems. We have calculated that PTF has the capability to significantly increase the number of such systems and potentially find many more systems with less regular outbursts. Additional discoveries would expand our understanding of both the structure and evolution of AM CVn systems and their population density.

Observations obtained with the Samuel Oschin Telescope at the Palomar Observatory as part of the Palomar Transient Factory project, a scientific collaboration between the California Institute of Technology, Columbia University, Las Cumbres Observatory, the Lawrence Berkeley National Laboratory, the National Energy Research Scientific Computing Center, the University of Oxford, and the Weizmann Institute of Science. Some of the data presented herein were obtained at the W. M. Keck Observatory, which is operated as a scientific partnership among the California Institute of Technology, the University of California, and the National Aeronautics and Space Administration. The Observatory was made possible by the generous financial support of the W. M. Keck Foundation. The William Herschel Telescope is operated on the island of La Palma by the Isaac Newton Group in the Spanish Observatorio del Roque de los Muchachos of the Instituto de Astrofísica de Canarias. This paper uses observations obtained with facilities of the Las Cumbres Observatory Global Telescope. The Byrne Observatory at Sedgwick (BOS) is operated by the Las Cumbres Observatory Global Telescope Network and is located at the Sedgwick Reserve, a part of the University of California Natural Reserve System.

S.B.C. acknowledges generous support from Gary and Cynthia Bengier, the Richard and Rhoda Goldman Fund, National Aeronautics and Space Administration (NASA)/*Swift* grant NNX10AI21G, NASA/*Fermi* grant NNX1OA057G, and National Science Foundation (NSF) grant AST–0908886.

Facilities: PO:1.2m, PO:1.5m, LCOGT, FTN (Spectral), Hale (DBSP), ING:Herschel (ACAM), Keck:I (LRIS)

REFERENCES

Abbott, T. M. C., Robinson, E. L., Hill, G. J., & Haswell, C. A. 1992, ApJ, 399, 680
Anderson, S. F., Becker, A. C., Haggard, D., et al. 2008, AJ, 135, 2108
Anderson, S. F., Haggard, D., Homer, L., et al. 2005, AJ, 130, 2230
Benn, C., Dee, K., & Agócs, T. 2008, in Ground-based and Airborne Instrumentation for Astronomy II, ed. I. S. McLean & M. M. Casali, Proc. SPIE, 7014, 70146X
Bertin, E., & Arnouts, S. 1996, A&AS, 117, 393
Bildsten, L., Shen, K. J., Weinberg, N. N., & Nelemans, G. 2007, ApJ, 662, L95
Bildsten, L., Townsley, D. M., Deloye, C. J., & Nelemans, G. 2006, ApJ, 640, 466
Buat-Ménard, V., & Hameury, J. 2002, A&A, 386, 891
Cenko, S. B., Fox, D. B., Moon, D.-S., et al. 2006, PASP, 118, 1396
Copperwheat, C. M., Marsh, T. R., Littlefair, S. P., et al. 2011, MNRAS, 410, 1113
Faulkner, J., Flannery, B. P., & Warner, B. 1972, ApJ, 175, L79
Fontaine, G., Brassard, P., Green, E. M., et al. 2011, ApJ, 726, 92
Groot, P. J., Nelemans, G., Steeghs, D., & Marsh, T. R. 2001, ApJ, 558, L123
Honeycutt, R. K. 1992, PASP, 104, 435
Horne, K. 1986, PASP, 98, 609
Kato, T., Nogami, D., Baba, H., Hanson, G., & Poyner, G. 2000, MNRAS, 315, 140
Kato, T., Reszelski, M., Poyner, G., et al. 2001, Inf. Bull. Var. Stars, 5120, 1
Lang, D., Hogg, D. W., Mierle, K., Blanton, M., & Roweis, S. 2010, AJ, 139, 1782
Law, N. M., Kulkarni, S. R., Dekany, R. G., et al. 2009, PASP, 121, 1395
Marsh, T. R. 1989, PASP, 101, 1032
Marsh, T. R., Dhillon, V. S., Littlefair, S. P., et al. 2007, in ASP Conf. Ser. 372, 15th European Workshop on White Dwarfs, ed. R. Napiwotzki & M. R. Burleigh (San Francisco, CA: ASP), 431
McCarthy, J. K., Cohen, J. G., Butcher, B., et al. 1998, Proc. SPIE, 3355, 81
Nather, R. E., Robinson, E. L., & Stover, R. J. 1981, ApJ, 244, 269
Naylor, T. 1998, MNRAS, 296, 339
Nelemans, G. 2005, in ASP Conf. Ser. 330, The Astrophysics of Cataclysmic Variables and Related Objects, ed. J.-M. Hameury & J.-P. Lasota (San Francisco, CA: ASP), 27
Nelemans, G., Portegies Zwart, S. F., Verbunt, F., & Yungelson, L. R. 2001, A&A, 368, 939
Nelemans, G., Yungelson, L. R., & Portegies Zwart, S. F. 2004, MNRAS, 349, 181
Nelemans, G., Yungelson, L. R., van der Sluys, M. V., & Tout, C. A. 2010, MNRAS, 401, 1347
Nogami, D., Monard, B., Retter, A., et al. 2004, PASJ, 56, L39
Ofek, E. O., Frail, D. A., Breslauer, B., et al. 2011, ApJ, in press (arXiv:1103.3010)
Osaki, Y. 1996, PASP, 108, 39
Paczyński, B. 1967, Acta Astron., 17, 287
Patterson, J., Kemp, J., Harvey, D. A., et al. 2005, PASP, 117, 1204
Patterson, J., Kemp, J., Shambrook, A., et al. 1997, PASP, 109, 1100
Patterson, J., Walker, S., Kemp, J., et al. 2000, PASP, 112, 625
Provencal, J. L., Winget, D. E., Nather, R. E., et al. 1997, ApJ, 480, 383
Rau, A., Kulkarni, S. R., Law, N. M., et al. 2009, PASP, 121, 1334
Rau, A., Roelofs, G. H. A., Groot, P. J., et al. 2010, ApJ, 708, 456
Reegen, P. 2007, A&A, 467, 1353
Roelofs, G. H. A., Groot, P. J., Marsh, T. R., Steeghs, D., & Nelemans, G. 2006a, MNRAS, 365, 1109
Roelofs, G. H. A., Groot, P. J., Marsh, T. R., et al. 2005, MNRAS, 361, 487
Roelofs, G. H. A., Groot, P. J., Nelemans, G., Marsh, T. R., & Steeghs, D. 2006b, MNRAS, 371, 1231
Roelofs, G. H. A., Groot, P. J., Nelemans, G., Marsh, T. R., & Steeghs, D. 2007a, MNRAS, 379, 176
Roelofs, G. H. A., Groot, P. J., Steeghs, D., et al. 2009, MNRAS, 394, 367
Roelofs, G. H. A., Nelemans, G., & Groot, P. J. 2007b, MNRAS, 382, 685
Sackett, P. D. 1997, ApJ, 483, 103
Schoembs, R., & Hartmann, K. 1983, A&A, 128, 37
Shears, J., Brady, S., Koff, R., Goff, W., & Boyd, D. 2011, arXiv:1104.0107
Shporer, A., Brown, T., Lister, T., et al. 2010, arXiv:1011.6394
Smak, J. 1967, Acta Astron., 17, 255
Solheim, J. 2010, PASP, 122, 1133
van Dokkum, P. G. 2001, PASP, 113, 1420
Warner, B. 1995, Cataclysmic Variable Stars (Cambridge: Cambridge Univ. Press)
Wood, M. A., Casey, M. J., Garnavich, P. M., & Haag, B. 2002, MNRAS, 334, 87
Woudt, P. A., Warner, B., & Rykoff, E. 2005, IAU Circ., 8531, 3